Sensors and Actuators B 204 (2014) 96–101

Contents lists available at ScienceDirect

Sensors and Actuators B: Chemical

journal homepage: www.elsevier.com/locate/snb

Dependence of Al^{3+} on the growth mechanism of vertical standing ZnO nanowalls and their NO_2 gas sensing properties

Lingmin Yu[a,*], Jiansong Wei[a], Yuyang Luo[a], Yanlong Tao[a], Man Lei[a], Xinhui Fan[a,**], Wen Yan[a], Peng Peng[b]

[a] School of Material and Chemical Engineering, Xi'an Technological University, Xi'an Xuefu Middle Road No. 2, China
[b] 2D Carbon Tech Co., Ltd., Changzhou, China

ARTICLE INFO

Article history:
Received 27 May 2014
Received in revised form 14 July 2014
Accepted 20 July 2014
Available online 2 August 2014

Keywords:
ZnO nanowalls
Soft solution method
Gas sensing
NO_2

ABSTRACT

In the present work, vertically well-aligned of ZnO nanowalls were successfully obtained on ITO glass substrate via a facile two-step soft aqueous solution using $Zn(CH_3COO)_2{\cdot}2H_2O$ and $Al(NO_3)_3{\cdot}9H_2O$ as the source materials in seed solution. Results showed that Al^{3+} played a critical role in synthesizing ZnO nanowalls. The $ZnAl_2O_4$ buffer layer not only reduced the surface energy of ITO glass substrate but also supported easy nucleation for ZnO. The effect of growth aqueous solution on tailoring morphology was investigated. Moreover, gas sensors based on the vertical standing ZnO nanowall were fabricated to examine the responses to NO_2 (1–50 ppm). The ZnO nanowalls exhibited a good response toward 50 ppm NO_2 as high as 30 at the operating temperature of 220 °C. In addition, the ZnO nanowalls showed fast response (30 s) and recovery (48 s) time to NO_2. These results showed that the vertical standing ZnO nanowalls were promising for NO_2 sensor applications.

1. Introduction

Nitrogen dioxide (NO_2) is one of the main air pollutants with serious adverse effects on health and environment. It is of great importance and interest to develop gas-sensing materials to NO_2 with high response, fast response time and excellent selectivity. Two-dimensional (2D) ZnO nanowall with high surface-to-volume ratio area and porous structure has been suggested to be ideal materials for the nanodevices used in chemical sensors [1,2].

Great attention has been attracted on the growth of high quality ZnO nanowall and on studying their performance [3,4]. It was reported that ZnO nanowall could be synthesized by metal organic vapor deposition method (MOCVD)[5–7], thermal evaporation [8,9], pulsed laser deposition (PLD)[10], electrochemical deposition [11,12] and aqueous solution method [13,14]. Among these techniques, aqueous solution method (ASM) has been widely accepted for the synthesis of metal oxide thin film on various substrates under the mild temperature and low cost.

Al foil or Al thin film on the substrate were often employed in two-step ASM methods to prepare ZnO nanowalls in previous studies [15–17]. It was noted that Al element has a significant influence on the synthesis of ZnO nanowalls. However, to the best of our knowledge, no efforts were made to determine the influence of Al element on the growth mechanism of stratiform ZnO nanowalls.

In the present work, Zn^{2+} and Al^{3+} were used to controllably synthesize ZnO nanowalls and the effect of growth aqueous solution on tailoring the morphology was investigated in detail. The influence of Al^{3+} on the growth mechanism of layered ZnO nanowalls was analyzed for the first time. Furthermore, the reliable sensing performance on NO_2 gas was demonstrated by gas-sensing characterization system.

2. Experiments

2.1. Fabrication of microstructure sensor based on ZnO Nanowalls

The preparation of vertical standing ZnO nanowalls included the coating of ZnO seed layer on surface of ITO glass substrate and the growth of two-dimensional ZnO nanowall. First of all, 0.02 mol zinc acetate ($Zn(CH_3COO)_2{\cdot}2H_2O$) and 0.01 mol aluminum nitrate ($Al(NO_3)_3{\cdot}9H_2O$) were used as the starting material to deposit the ZnO seed layer on the ITO glass substrate [15]. It was important to note that Al^{3+} had a key role on the formation of ZnO nanowalls. Secondly, ZnO nanowalls thin films were subsequently grown on the ZnO seed layer by a facile process. Briefly, The growth aqueous

* Corresponding author. Tel.: +86 29 86173324; fax: +86 29 86173324.
** Corresponding author.
E-mail addresses: ylmyl@163.com (L. Yu), fanxh2002@xatu.edu.cn (X. Fan).

http://dx.doi.org/10.1016/j.snb.2014.07.071
0925-4005/

solution was prepared by zinc nitrate hexahydrate($Zn(NO_3)_2 \cdot 6H_2O$) and hexamethylene tetramine (HMT), with the concentration of zinc ions being 0.01 mol/L and the molar ratio of Zn^{2+} to HMT being as 1. Subsequently, a piece of substrate coated with seed film was placed vertically in growth solution and heated at a constant temperature of 353 K for 5 h. Finally, the thin film was rinsed by deionized water to remove residual salts, and dried in oven.

Morphology control of vertical standing ZnO nanowalls was achieved by varying the concentration of zinc ions in the growth aqueous solution among 0.01 mol/L, 0.05 mol/L and 0.075 mol/L.

2.2. Characterization and gas-sensing measurement

The sensor substrate area (Ag–Pd electrodes) was about 13.4 mm × 7 mm. The width of the signal Au–Pd strips was 300 μm, and the distance between the adjacent Au–Pd strips was also 100 μm (Fig. 1a). The gas-sensing properties of the sensors toward NO_2 gas were performed on a Chemical Gas Sensor-1 Temperature Pressure (CGS-1TP) intelligent gas sensing analysis system (Beijing Elite Tech Co., Ltd.). It is claimed offering an external temperature control from room temperature to 500 °C with an adjustment precision of 1 °C. As seen in Fig. 1b, two adjustable probes were pressed on the sensor electrodes to collect electrical signals. Electrical resistances in the air and in the tested gases were tested on a static system after the gas-sensing devices were aged at different operating temperatures for about 30 min. When the resistance value was stable, a certain concentration of NO_2 gas was injected into the testing chamber (18 L in volume) and heated, and then the saturated target gas was mixed with air by two fans. After its resistance value reached a new constant value, the test chamber was opened to recover the sensor in air. The sensor resistance and sensitivity were also collected and analyzed by the system in real time. The sensor response to a reducing gas was defined as the ratio of resistance of sample in the air (R_a) to its resistance in the test gas, i.e., $(R_g) \cdot S = R_a/R_g$. The time taken by the sensor resistance to change from R_a to $R_a - 90\% \times (R_a - R_g)$ was defined as response time when the target gas was introduced to the sensor, and the time taken from R_g to $R_g + 90\% \times (R_a - R_g)$ was defined as recovery time when the ambience was replaced by air.

The general morphology, crystal structure of these nanostructures were characterized using scanning electron microscopy (SEM) (FEI Quanta 400 FEG), high-resolution transmission electron microscopy (HRTEM, JEM-2010) at 400 kV, powder crystal X-ray diffractometer (XRD-6000) using Cu Kα radiation (λ = 1.54056 Å). The elemental composition was obtained by an energy-dispersive X-ray spectrometer (EDS) attached to the SEM.

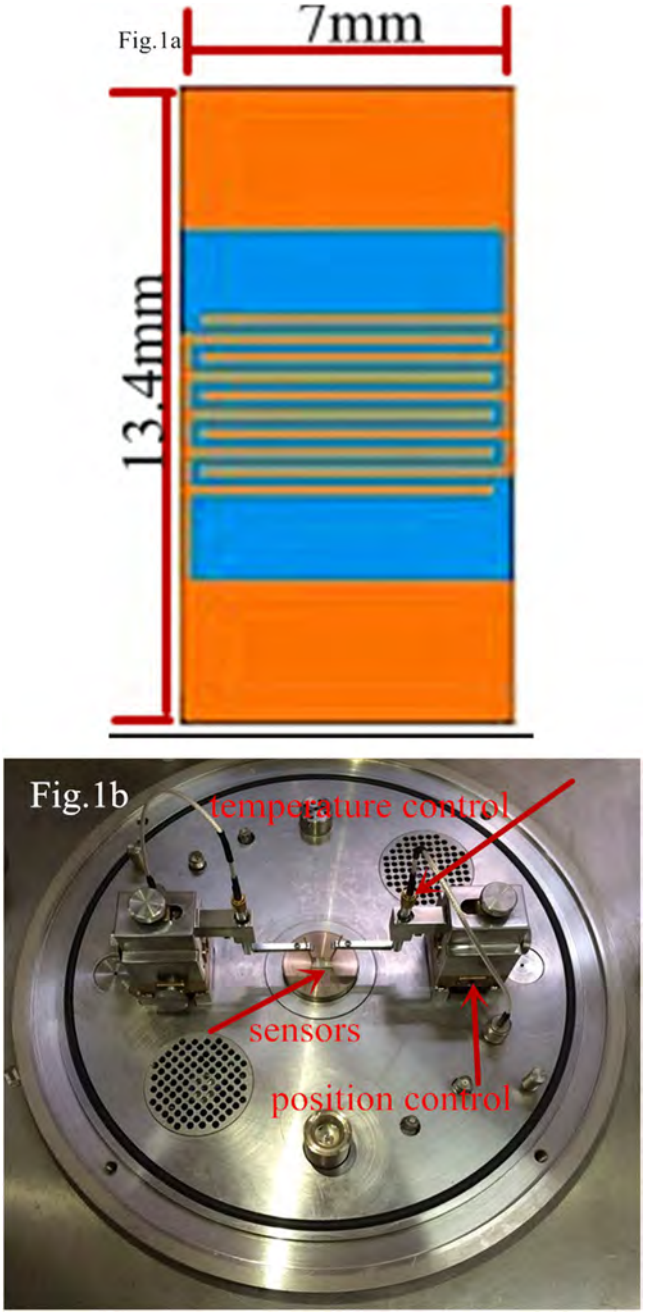

Fig. 1. (a) Schematic diagram of sensor electrode substrates (b) a photograph of gas sensing analysis system.

3. Results and discussions

The morphologies of the three samples were observed by SEM at different magnifications, as shown in Fig. 2. Low magnification image (Fig. 2a) for sample 1 confirmed that nanowalls with high reproducibility were uniformly distributed on ITO glass substrate surface. Under close inspection (Fig. 2b), it indicated the geometrical shape of nanowall presented thin nanosheets in microns length and ~20 nm thickness. Though most of the sheets were exhibited a little tilting angles, the figurations were regular. When the concentration of zinc ions in the growth aqueous solution decreased to 0.05 mol/L^{-1} (sample 2), it was noted that dense nanodisks, without titling, stood perpendicularly on the substrate (Fig. 2c). In Fig. 2d, it was found that the thicknesses and the length of the vertically standing ZnO nanodisks were about ~80 nm and ~1 μm, respectively. For the sample 3, a dense structure continually improved with the 0.075 mol/L zinc ions concentration in the growth solution, as shown in Fig. 2e and f. In Fig. 2e, it was shown that up-right standing nanowalls were interconnected at different tilting angles. The as grown nanowalls were with homogenous length range between 1–1.5 μm and widths between 50–60 nm. All of these walls were interconnected to form a mesoporous structure, which could provide a continuous path for charge carriers with much less grain boundaries and thus presented effective gas sensing properties [16]. For further element analysis, EDX (energy dispersive X-ray spectroscopy) attached to SEM were carried out. The corresponding spectrum was shown in the inset of Fig. 2f. It showed the featured aluminum peak, while as expected the zinc and oxygen peaks were very dominant. The spectrum suggested that aluminum could be found in the ZnO structures.

The sensor substrates were subjected to the same synthesis treatment as sample 3, selective coatings of Ag–Pd interdigitated

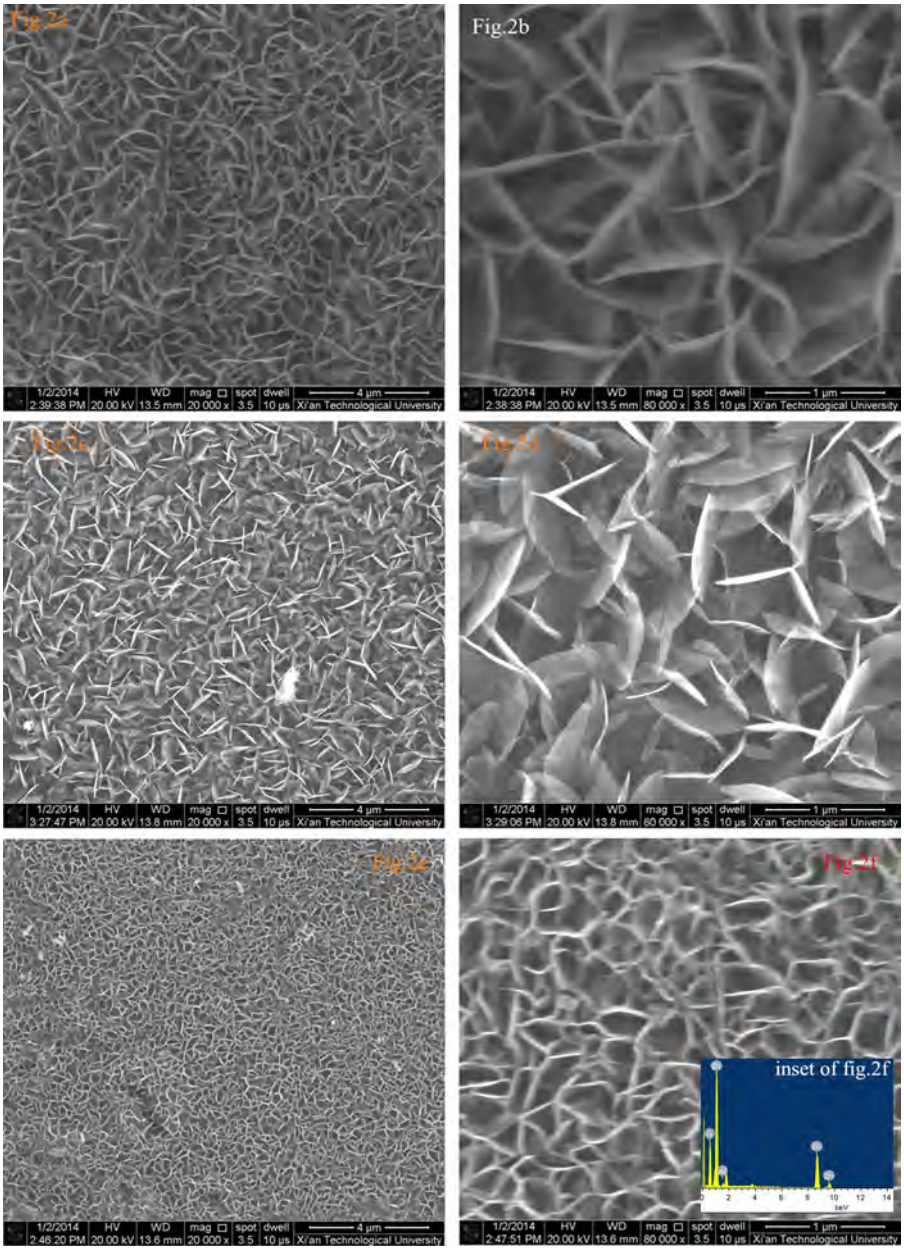

Fig. 2. Different magnification SEM images dependence of the zinc iron in growth solution (a–b) 0.01 mol mol^{-1}, (c–d) 0.05 mol mol^{-1}, (e–f) 0.075 mol mol^{-1}, and the inset in Fig. 1f is the EDX spectra of ZnO nanowalls for sample 3.

electrodes for synthesis of patterned ZnO nanowalls were shown in Fig. 3. There were three pairs of Ag–Pd interdigitated electrodes on the sensor substrate. The ZnO nanowalls exhibited the same significant morphological smoothness on Ag–Pd electrodes as that of ITO glass substrate.

Fig. 4 showed the X-ray diffraction pattern of the three samples on ITO glass substrate. A strong diffraction peak of the nanowalls appeared at around $2\theta = 34.5^{\circ}$, which corresponded to wurtzite structure zinc oxide (0 0 0 2) peak (PDF#36-1451). However, other peaks were vary weaker, indicating that the ZnO nanowalls were well crystallized and grown along the [0 0 1] direction. In addition, no diffraction peaks from Zn or other phases were observed, suggesting their good structural properties.

Further structure characterization of ZnO nanowalls for the sample 2 was performed by TEM and SAED pattern, respectively. As shown in Fig. 5a, nanowalls in the present work appeared to single layer with semicircular disk shape. In addition, it could be seen from Fig. 5a that the ZnO nanowall was smooth and homogeneous in thickness. A well-ordered crystal lattice array without structural defects was observed, as illustrated in the high-resolution TEM image of individual ZnO nanodisks (Fig. 5b). The lattice spacing between the adjacent planes was measured to be 0.26 nm, corresponding to the d-spacing of ZnO (0 0 0 2) planes. The single-crystalline nature of the ZnO nanowall networks was also confirmed from the ordered dots arrays SAED patterns, shown in the inset of Fig. 5b. Together with the corresponding HRTEM patterns, we figured out that these single-crystalline ZnO nanowall networks with few crystal defects, offering high-quality conduction channels for electrical nanodevices.

The effect of Al^{3+} on the vertical standing growth of the ZnO nanowalls was investigated. It was well known that ZnO nanoseed was used to acquire by the hydrolysis of $ZnAc_2 \cdot 2H_2O$ and

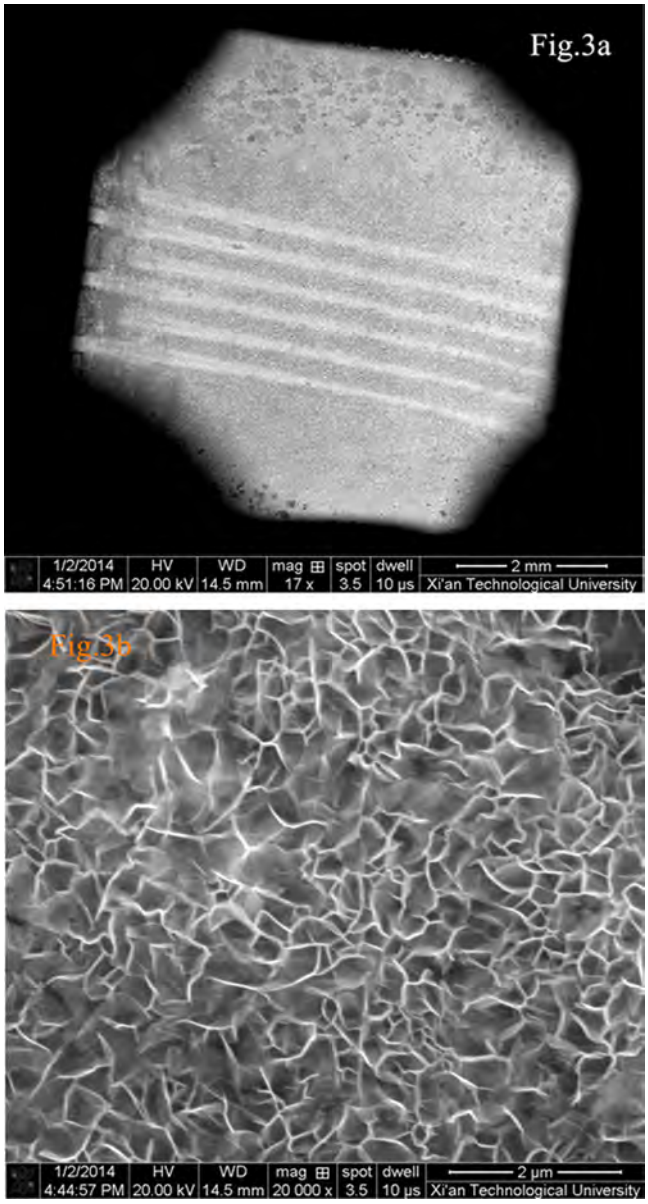

Fig. 3. Selective deposition of ZnO nanowalls on Ag–Pd electrodes (a) low magnification, (b) high magnification.

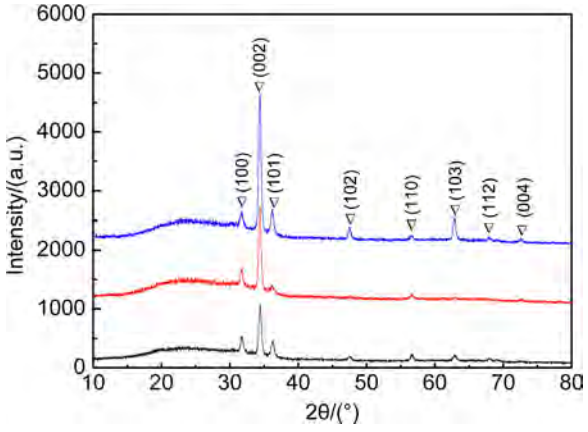

Fig. 4. XRD pattern of ZnO nanowall.

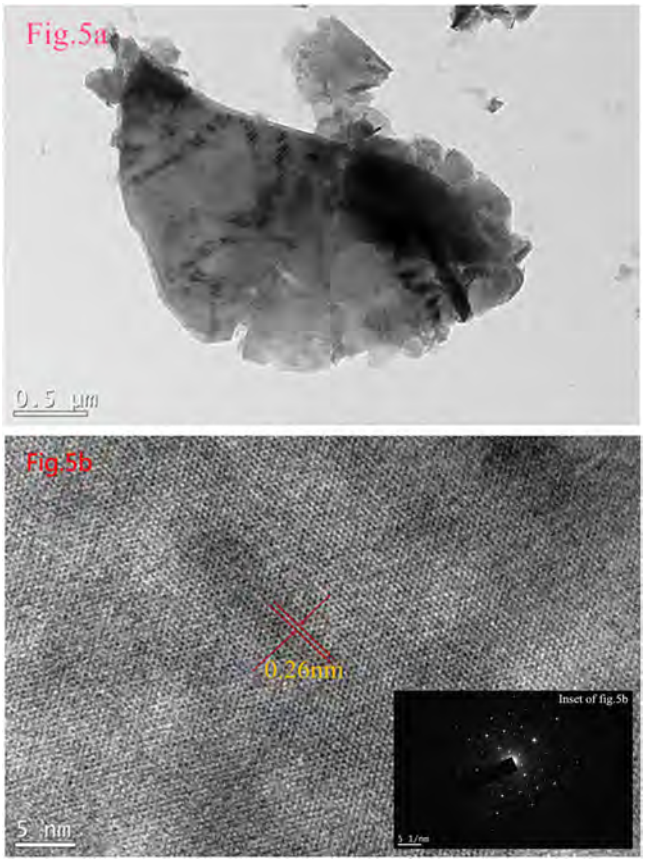

Fig. 5. (a) Low-magnification cross-sectional TEM image of individual ZnO nanowalls, (b) High-resolution TEM image of individual ZnO nanowalls. The inset is a selected-area electron diffraction (SAED) pattern.

$Al(NO_3)_3{\cdot}9H_2O$. The possible chemical reaction is illustrated in Eqs. (1)–(11).

$$(CH2)_6N4 + 6H_2O \rightarrow 4NH_3 + 6HCHO \quad (1)$$

$$NH_3 + H_2O \rightarrow NH_4^+ + OH^- \quad (2)$$

$$ZnAc_2{\cdot}2H_2O \rightarrow Zn^{2+} + 2Ac^- + 2H_2O \quad (3)$$

$$Al(NO_3)_3{\cdot}9H_2O \rightarrow Al^{3+} + 3NO_3^- + 9H_2O \quad (4)$$

$$Zn^{2+} + 2OH^- \rightarrow Zn(OH)_2 \quad (5)$$

$$Al^{3+} + 3OH^- \rightarrow Al(OH)_3 \quad (6)$$

$$Al(OH)_3 + OH^- \rightarrow AlO_2^- + 2H_2O \quad (7)$$

$$Zn(OH)_2 + 2OH^- \rightarrow [Zn(OH)_4]^{2-} \quad (8)$$

$$Zn^{2+} + AlO_2^- \rightarrow ZnAl_2O_4 \quad (9)$$

$$[Zn(OH)_4]^{2-} + Zn^{2+} \rightarrow 2Zn(OH)_2 \quad (10)$$

$$Zn(OH)_2 \rightarrow ZnO + H_2O \quad (11)$$

In fact, there was a certain competition due to the difference of solubility product for $Al(OH)_3$($K_{sp} = 3 \times 10^{-34}$) and $Zn(OH)_2$ ($K_{sp} = 3 \times 10^{-17}$), which resulted in the preferential precipitation of potential $Al(OH)_3$. As a result, Eq. (6) allowed for the formation of AlO_2^- [17]. Then, the anion AlO_2^- was liable to be adsorbed by the Zn^{2+} ions on the positive polar (0 0 0 1) and followed by Eqs. (5), (8), (10) and (11) to form ZnO nuclei[18]. As buffer layer, $ZnAl_2O_4$ reduced the surface energy of ITO glass and then supported more easily nucleation for ZnO. In addition, $[Zn(OH)_4]^{2-}$ was defined to layered hydroxy salts (Zn-LHS) while stratiform metal oxide was obtained easily by the transformation of Zn-LHS.

Table 1
Comparison of ZnO nanowall sensors in this work with those reported in the literatures.

Structure	Synthesis method	NO_2 (ppm)	Sensitivity (R_g/R_a)	Operating temperature (°C)	Response/ recovery time (s)	References
ZnO nanowalls	A facile two-step soft aqueous solution	50	30	220	30/48	This work
Flower-like ZnO microstructures (5–7 μm)	Hydrothermal method	100	12.27	300	–	[20]
ZnO hollow spheres	Carbon microspheres as templates	50	172.8	240	19	[21]
ZnO nanoparticles (23.2 nm)	Annealing the precursor of zinc carbonate hydroxide	40	220	290	30/120	[22]
Necked ZnO nanoparticle	Purchased from Sigma–Aldrich Inc.	5	400	200	13/10	[23]
Porous ZnO polygonal nanoflakes	Microwave hydrothermal method	5	560	175	–	[24]
ZnO coatings	Atmospheric plasma-sprayed	2.42	5.3	300	–	[25]
ZnO nanowire	Carbothermal reduction process	5	55	225	44/5	[26]

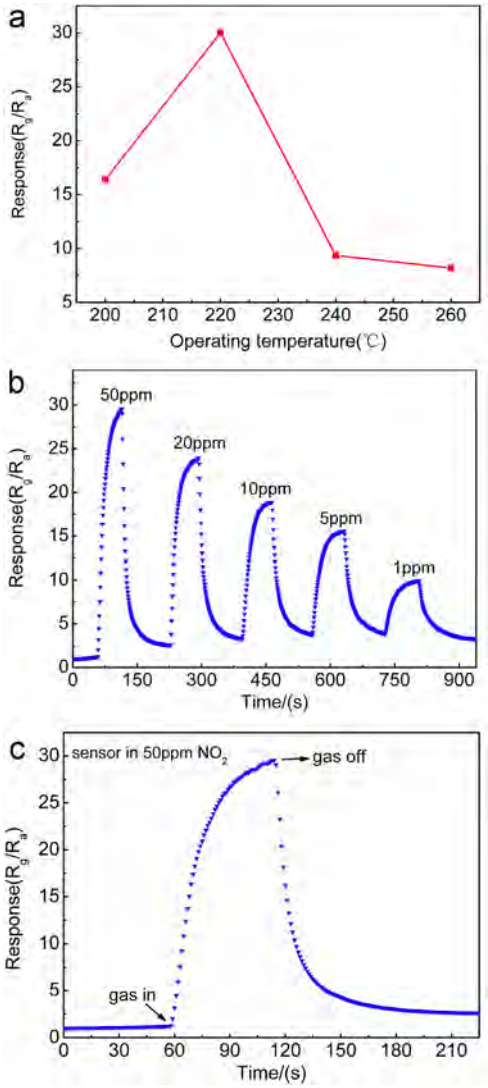

Fig. 6. (a) Gas response of ZnO nanowalls to 50 ppm as the function of the operating temperature and (b) response transients of the ZnO nanowall to different concentration of NO_2, (c) response–recovery time curve of ZnO nanowalls to 50 ppm NO_2.

Recently, semiconductor oxides materials with porous architectures are considered to be ideal structure for the gas-sensing applications due to their high surface area. To investigate the NO_2 sensing properties of ZnO nanowall for the sample 3, sensor was tested at different temperatures ranging from 200 °C to 260 °C respectively for NO_2 to get the optimize working temperature, which retained the equilibration between the diffusion of gas molecules and the absorbed oxygen species [19]. Fig. 6a showed the gas response measured for sample 2–50 ppm NO_2 in air. It could be seen from curves in Fig. 6a, the ZnO nanowall exhibited the highest response of 30 at operating temperature of 220 °C. Fig. 6b showed the response and recovery behaviors of the sensor upon being orderly exposed to 1–50 ppm NO_2. In the measurements, the responses were 10.14, 15.81, 19.02, 24.1, and 30.0 to 1, 5, 10, 20, 50 ppm NO_2, respectively. The gas response–recovery time curves of vertical standing ZnO nanowalls sensors to 50 ppm NO_2 were shown in Fig. 6c, it exhibited fast response and recovery to NO_2 at operating temperature of 220 °C. The response and recovery time of ZnO nanowall sensor were 30 s and 48 s, respectively. The above results revealed that vertical-standing growth of ZnO nanowalls were promising candidates for high performance gas sensors. However, facile applications of vertical-standing ZnO nanowalls as the functional film still need further investigation.

The NO_2 sensing performance of ZnO based with different morphologies were summarized in Table 1, as given in Refs. [20–26]. From the comparison, one could conclude that the NO_2 sensor based on vertical standing ZnO nanowall showed a fast response–recovery time and intermediate gas response to NO_2 at lower operating temperature.

It was found that the gas-sensing properties of ZnO nanostructures were greatly dependent on the size of the structures. The size of flower-like ZnO microstructures [21] was about 5–7 μm in radius and their gas response to 100 ppm NO_2 was as low as 12.27. In contrast, nanoparticles with average size of 23.2 nm showed a high sensitivity (2 2 0) against 40 ppm NO_2. In our work, the thicknesses and length of the vertically standing ZnO nanodisks were ~80 nm and ~1 μm. According to the above data, the experimental results of ZnO nanowall sensors supported D–L model [27].

On the other hand, the response and recovery time were attributed to the unique device structure[26]. When ZnO nanostructures as a solid film in the sensor were floated or distributed above the substrate, the adsorbed molecules could be easily desorbed and swepted away from the surface of ZnO. In the typical ZnO nanowall-based gas sensors, multiple ZnO nanowalls were grown from the substrate and had a solid connection with it, thus gas molecules adsorbed between the nanowalls and the substrate would require longer time to be desorbed from the surface of ZnO resulting a slow recovery. However, the mesoporous structure could provide a continuous path for charge carriers owing to much less grain boundaries and thus presented faster response time.

4. Conclusion

We have demonstrated the effect of the growth aqueous solution on tailoring morphology of ZnO nanowalls using two-step solution methods. The ZnO nanowalls morphology was found to be controllable by processing conditions such as growth solution. The results showed that the vertical standing of ZnO nanowall networks were well crystallized in a wurtzite structure and highly oriented direction parallel to [0 0 0 1]. It is found that Al^{3+} is crucial to

growing ZnO nanowalls, which results in the formation of $ZnAl_2O_4$ that leads to vertical growth of ZnO nanowalls with sheet geometrical shape. In addition, the ZnO nanowalls were used to fabricate gas sensors with good NO_2 sensing properties. Under optimize working temperature 220 °C, the sensor based on ZnO nanowall showed high response 30–50 ppm NO_2 due to the porous structure, highly exposed surface area and singe-crystal structure. The results well illustrated that the controlling of the structure of ZnO nanowall films was an effective way to meet the needs of ZnO devices with good performances.

Acknowledgments

The research was supported by National Natural Science Foundation of China (Grant nos. 51072156 and 51202177) and Science & Research Fund of Education Commission of Shaanxi Province (No. 2013JK0930).

References

[1] T.N. Hou, L. Jun, K.S. Michael, N. Pho, C. Alan, H. Jie, M. Meyyappan1, Growth of epitaxial nanowires at the junctions of nanowalls, Science 300 (2003) 1249.
[2] C.H. Lee, Y.J. Kim, J. Lee, Y.J. Hong, J.M. Jeon, M. Kim, S. Hong, G.C. Yi, Scalable network electrical devices using ZnO nanowalls, Nanotechnology 22 (2011) 055205–055211.
[3] J.P. Cheng, X.B. Zhang, Z.Q. Luo, Oriented growth of ZnO nanostructures on Si and Al substrates, Surf. Coat. Technol. 202 (2008) 4681–4686.
[4] H.H. Huang, H.N. Wang, B. Li, X.M. Mo, H. Long, Y. Li, H. Zhang, D.L. Carroll, G.J. Fang, Seedless synthesis of layered ZnO nanowall networks on Al substrate for white light electroluminescence, Nanotechnology 24 (2013) 315203–315209.
[5] S.-W. Kim, Catalyst-free synthesis of ZnO nanowall networks on Si3N4/Si substrates by metal organic chemical vapor deposition, Appl. Phys. Lett. 88 (2006) 253114.
[6] C.C. Wu, D.S. Wuu, P.R. Lin, T.N. Lin, N. Chen, R.H. Horng, Effects of growth conditions on structural properties of ZnO nanostructures on sapphire substrate by metal–organic chemical vapor deposition, Nanoscale Res. Lett. 23 (2009) 377–384.
[7] J.H. Lee, D.C. Kim, S.Y. Kim, Microstructural characterization and formation mechanism of 211 top facets of ZnO-based nanowall structures, Physica B 412 (2013) 12–16.
[8] Z. Yin, N. Chen, On the formation of well-aligned ZnO nanowall networks by catalyst-free thermal evaporation method, J. Cryst. Growth 305 (2007) 296–301.
[9] T.P. Chen, S.P. Chang, F.Y. Hung, S.J. Chang, Simple fabrication process for 2D ZnO nanowalls and their potential application as a methane sensor, Sensors 13 (2013) 3941–3950.
[10] C. Li, G.C. Li, G.J. Fang, Q. Fu, Effect of substrate temperature on the growth and photoluminescence properties of vertically aligned ZnO nanostructures, J. Cryst. Growth 292 (2006) 19–25.
[11] D. Pradhan, M. Kumar, Y. Ando, K.T. Leung, Efficient field emission from vertically grown planar ZnO nanowalls on an ITO–glass substrate, Nanotechnology 19 (2008) 035603.
[12] D. Pradhan, S.K. Mohapatra, Morphology-controlled ZnO nanomaterials for enhanced photoelectrochemical performance, Mater. Expr. 1 (2011) 59–67.
[13] J.P. Cheng, Z.M. Liao, D. Shi, F. Liu, X.B. Zhang, Oriented ZnO nanoplates on Al substrate by solution growth technique, J. Alloys Compd. 480 (2009) 741–746.
[14] D.H. Kim, S.D. Lee, K.K. Kim, G.S. Park, J.M. Lee, S.W. Kim, Free-standing ZnO nanorods and nanowalls by aqueous solution method, J. Nanosci. Nanotechnol. 8 (2008) 4688–4691.
[15] X. Yan, X. Tong, J. Wang, C. Gong, Controllable synthesis of three-dimensional hierarchical porous ZnO film with mesoporous nanowalls, Mater. Lett. 92 (2013) 165–168.
[16] Z.Q. Liang, R. Gao, J.L. Lan, Growth of vertically aligned ZnO nanowalls for inverted polymer solar cells, Sol. Energy Mater. Sol. Cells 117 (2013) 34–40.
[17] M. Kashif, M. Syed, A. Usman, K.L. Foo, U. Hashim, M. Willander, ZnO nanoporous structure growth, optical and structural characterization by aqueous solution route, AIP Conf. Proc. 1341 (2011) 92–95.
[18] Y. Lingmin, X.-H. Fan, J.-Y. Shui, L. Cao, W. Yan, Research on the growth of ZnO nanowall by soft-solution route, Mater. Lett. 68 (2012) 423–425.
[19] Y. Lingmin, F. Xinhui, C. Lei, Q. Lijun, Y. Wen, Gas sensing enhancement of aluminum-doped ZnO nanovase structure with many gas facile diffusivity paths, Appl. Surf. Sci. 265 (2013) 108–113.
[20] P. Rai, S. Raj, K.-J. Ko, K.-K. Park, Y.-T. Yu, Synthesis of flower-like ZnO microstructures for gas sensor applications, Sens. Actuators B 178 (2013) 107–112.
[21] J. Zhang, S. Wang, Y. Wang, M. Xu, X. Guo, S. Wu, ZnO hollow spheres: preparation, characterization, and gas sensing properties, Sens. Actuators B 139 (2009) 411–417.
[22] F. Fan, Y. Feng, S. Bai, D. Li, Synthesis and gas sensing properties to NO_2 of ZnO nanoparticles, Sens. Actuators B 185 (2013) 377–382.
[23] J.H. Jun, J. Yun, K. Cho, S. Kim, Necked ZnO nanoparticle-based NO_2 sensors with high and fast response, Sens. Actuators B 140 (2009) 412–417.
[24] M. Chen, Z. Wang, D. Han, F. Gu, G. Guo, Porous ZnO polygonal nanoflakes: synthesis, use in high-sensitivity NO_2 gas sensor, and proposed mechanism of gas sensing, J. Phys. Chem. C 115 (2011) 12763–12773.
[25] C. Zhang, M. Debliquy, H. Liao, Deposition and microstructure characterization of atmospheric plasma-sprayed ZnO coatings for NO_2 detection, Appl. Surf. Sci. 256 (2010) 5905–5910.
[26] M.-W. Ahn, K.-S. Park, J.-H. Heo, D.-W. Kim, K.J. Choi, On-chip fabrication of ZnO-nanowire gas sensor with high gas sensitivity, Sens. Actuators B 138 (2009) 168–173.
[27] M. Chen, Z. Wang, D. Han, F. Gu, Porous ZnO polygonal nanoflakes: synthesis, use in high-sensitivity NO_2 gas sensor, and proposed mechanism of gas sensing, J. Phys. Chem. C 115 (2011) 12763–12773.

Biographies

Lingmin Yu received her PHD degree from Xi'an Jiao Tong University in 2010. Now, she has been working as associate professor in Xi'an Technological University. She focuses on developing layered functional nanomaterials for gas sensors. Her research project involves nanomaterials (ZnO, graphene and MoS_2) sensing materials.

Jiansong Wei received her bachelor's degree from Guangxi University for Nationalities and is currently pursuing a MS degree at Xi'an Technological University. His research project involves sensing materials.

Yuyang Luo received his bachelor's degree from Xi'an Technology University. His research project involves sensing materials.

Yanlong Tao received his bachelor's degree from Xi'an Technology University. His research project involves sensing materials.

Man Lei received her master's degree from Xi'an Technological University. Her research project involves sensing materials.

Xinhui Fan received PHD in North Western Polymer University in 1997. His research interests are in the field of sensors, he is presently a professor and doctoral tutor in Xi'an Technological University.

Wen Yan received PHD in University of Manchester. His research interests are in the field of sensors, he is presently a professor and doctoral tutor in Xi'an Technological University.

Peng Peng received PHD in University of Houston in 2006.